General Disclaimer

One or more of the Following Statements may affect this Document

- This document has been reproduced from the best copy furnished by the organizational source. It is being released in the interest of making available as much information as possible.

- This document may contain data, which exceeds the sheet parameters. It was furnished in this condition by the organizational source and is the best copy available.

- This document may contain tone-on-tone or color graphs, charts and/or pictures, which have been reproduced in black and white.

- This document is paginated as submitted by the original source.

- Portions of this document are not fully legible due to the historical nature of some of the material. However, it is the best reproduction available from the original submission.

Produced by the NASA Center for Aerospace Information (CASI)

X-692-71-66

REPRINT

NASA TM X- 65489

REVERSE AND FORWARD SLOW SHOCKS IN THE SOLAR WIND

L. F. BURLAGA

J. K. CHAO

RECEIVED
NASA STI FACILITY
INPUT BRANCH
MAY 1971

FEBRUARY 1971

GSFC

GODDARD SPACE FLIGHT CENTER

GREENBELT, MARYLAND

FACILITY FORM 602

N71 24166 (ACCESSION NUMBER) (THRU)

26 (PAGES) 63 (CODE)

TMX 65489 (NASA CR OR TMX OR AD NUMBER) 29 (CATEGORY)

X-692-71-66

REVERSE AND FORWARD SLOW SHOCKS IN THE SOLAR WIND

by

L. F. Burlaga
Laboratory for Extraterrestrial Physics
NASA Goddard Space Flight Center
Greenbelt, Maryland

and

J. K. Chao*
Center for Space Research
Massachusetts Institute of Technology
Cambridge, Massachusetts

March 1971

*Present Address: Laboratorio Plasma nello Spazio del CNR presso
Instituto di Fisica "G. Marconi"

Abstract

A reverse slow shock and a forward slow shock were found in plasma and magnetic field data from Pioneer 6. The shocks were oblique and weak (Mach ≈ 1.2).

Numerous non-shock-like discontinuities were found with $B_1 \neq B_2$ and $n_1 \neq n_2$. Assuming pressure balance across them, we obtained an average electron temperature $T_e = (1.8 \pm .2) \times 10^5 {}^oK$. It was observed that discontinuities with $B_1 \neq B_2$, $n_1 = n_2$ seldom if ever occur.

I. Introduction

Recently, a reverse perpendicular fast shock (Burlaga, 1970) and two forward slow shocks (Chao and Olbert, 1970) were identified in the solar wind. There is also some evidence for a reverse oblique fast shock (Chao and Binsak, 1971). Reverse slow shocks have not hitherto been reported.

We have scanned Pioneer 6 data in seach of such shocks with the aim of confirming and extending the above results. The search is described in Section II and the results are discussed in Section III. Numerous discontinuities were found which are not shocks. From these we obtained an estimate of the average solar wind electron temperature which is independent of spacecraft sheath effects (Section IV).

The data used in this study are from Pioneer 6 which was launched on December 15, 1965 into a heliocentric orbit with apogee .98 AU and perigee .82 AU. A plot of its orbit during the early days of the flight, which turn out to be the times of interest, may be found in Ness (1966). The magnetic field data were obtained by Ness and the plasma data by Bridge, Lazarus, and Davis. A discussion of their instruments may be found in Ness et al. (1966) and Lazarus et al. (1966), respectively.

II. Selection of Discontinuities

The search for shocks was begun by looking for discontinuities in the magnetic field intensity B, since a jump in B is a necessary condition for all shocks except a parallel shock and since B is measured more frequently than the plasma parameters. A quantitative criterion for selecting changes in B was not used, since the variations in B are very complex. Instead, they were selected subjectively with an attempt to choose mostly step-like changes, the change being $\pm 20\%$ in $\lesssim 1$ min and the field intensity being nearly uniform over the 5 min intervals before and after the change. Plasma data were not available for all of these discontinuities. The results that follow concern only those discontinuities for which both plasma and magnetic field data are available.

To isolate the shocks, we first selected those discontinuities which had the correct signature (Colburn and Sonett, 1966), then eliminated those which clearly did not satisfy the Rankine-Hugoniot equations using the fitting scheme of Chao (1970), and finally eliminated those discontinuities which could conceivably satsify the pressure balance condition for tangential and rotational discontinuities. Discontinuities which were not shocks were considered spearately and were used to obtain the electron temperature as discussed in Section IV.

The distribution of B for the discontinuities which were selected from Pioneer 6 data for this study is shown at the top of Figure 1. The absence of discontinuities near B = 0 is due to our selection criterion. The corresponding distributions of density changes and thermal speed changes are also shown in Figure 1. The changes in n were <10% for less than 5% of the discontinuities. This has implications concerning some results presented recently by Ivanov (1970).

Ivanov pointed out that in an anisotropic plasma, the hydromagnetic equations allow the existance of a kind of discontinuity with the following characteristics: 1) there is a mass flux through the surface, 2) the magnetic field intensity changes across the surface while the density is the same on both sides of the surface, 3) there is a component of B normal to the surface, and 4) the components of B parallel to the surface are themselves parallel. He calls this a "rotational" discontinuity but this term is misleading since the tangential component of $\underset{\sim}{B}$ does not rotate. In fact, it is more like a "shock" for which $n_1 = n_2$ in the sense that it satisfies the coplanarity theorem and other shock equations. Figure 1, shows that <5% of the discontinuities which are identified in Pioneer 6 data satisfy the condition $B_1 \neq B_2$, $n_1 = n_2$ necessary for Ivanov's discontinuities. Thus, Ivanov's discontinuities occur infrequently if at all.

III. Slow Shocks

For a slow shock, the following conditions must be satisfied.

1) The measured 14 parameters, $\underset{\sim}{B}_1$, $\underset{\sim}{B}_2$, $\underset{\sim}{V}_1$, $\underset{\sim}{V}_2$, n_1 and n_2 must satisfy the Rankine-Hugoniot equations.

2) The computed Alfven Mach numbers, $M_A = V_n^*/V_A$ ahead and behind the shock must be both less than one, where V_n^* is the component of the bulk velocity normal to the shock front and measured in the shock frame of reference, and V_A is the Alfven speed based on the magnetic field component normal to the shock front.

3) The Mach numbers based on the slow mode of magnetosonic waves, $M_{slow} = V_n^*/V_{slow}$, must be larger than 1 ahead of the shock and less than 1 behind the shock; here V_{slow} is the speed of the slow mode of the magnetosonic wave in the direction of the shock normal. To compute V_{slow}, one must know the total pressure of the plasma. Although this pressure is not measured directly, it can be estimated from the conservation equations for the normal momentum flux and the energy flux.

4) The computed electron temperatures ahead and behind the shock should be reasonable, i.e., on the order of 1.5×10^5 °K.

(Montgomery et al., 1970; Hundhausen and Montgomery, 1971).

Besides showing that these conditions are satisfied, it is desirable to show that the events do not satisfy the pressure balance condition for tangential or rotational discontinuities.

A Reverse Slow Shock. Figure 2 shows a discontinuity which has the signature of a reverse slow shock, namely, a discontinuous decrease in n and T and a simultaneous increase in V and B. It was seen at Pioneer 6 at 0109 UT on January 19, 1966. Using the procedure described by Chao (1970), a set of 14 parameters was obtained ($\underset{\sim}{B}_1$, $\underset{\sim}{B}_2$, $\underset{\sim}{V}_1$, $\underset{\sim}{V}_2$, n_1,

and n_2, see Table 1) which satisfy the Rankine-Hugoniot equations for an isotropic plasma and which are close to the observed average values for the discontinuity. We use here the RTN coordinates in which the R axis is out from the sun and parallel to the sun-earth line, the T axis is in the direction of the motion of the earth, the R-T plane is parallel to the ecliptic, and the N-axis is northward and perpendicular to the ecliptic. These "theoretical" values are given in Table 1 and are shown by the solid lines in Figure 2. They are to be compared with the observed values shown in Figure 2. The close agreement shows that the observed parameters and changes are consistent with the Rankine-Hugoniot equations. Using the Rankine-Hugoniot equations, it is possible to solve for 3 of the 14 measured parameters as a function of the remaining 11 (Chao and Olbert, 1970). In particular, one can solve for $\underset{\sim}{V}_2$ as a function of ($\underset{\sim}{B}_1$, $\underset{\sim}{B}_2$, $\underset{\sim}{V}_1$, n_1, n_2). Then, the measured parameters $\underset{\sim}{B}_1$, $\underset{\sim}{B}_2$, $\underset{\sim}{V}_1$, n_1 and n_2 are allowed to vary independently within their uncertainties for computing the $\underset{\sim}{V}_2$ values. When the computed value of $\underset{\sim}{V}_2$ is within the uncertainties of its measured average value, then this computed value can be regarded as a prediction. Table 2 compares the "predicted" and observed values of $\underset{\sim}{V}_2$. The agreement is good. (See Figures 2, and 8 also).

The velocity of the shock surface relative to the spacecraft was found to be $\underset{\sim}{V}_s$=(212,1,135)km/sec, corresponding to a speed 251/km/sec and a shock normal $\hat{n}$=(0.85, 0.01, 0.54). The angle, $\theta_{\underset{\sim}{B}\cdot\hat{n}}$, between $\underset{\sim}{B}_1$ and $\hat{n}$ was found to be 42° as given in Table 3. Relative to the shock, the normal component of the flow velocity decreased from 29 km/sec to 23 km/sec (See Table 3). The Mach numbers M_A and M_{slow}, ahead and behind the shock are given in Table 4. They do satisfy the conditions for a slow shock, i.e. the flow is sub-alfvenic

on both sides of the shock, it is super-slow ahead of the shock and it is sub-slow behind the shock.

This discontinuity cannot be a tangential discontinuity with $T_{e_1} = T_{e_2}$, for the pressure balance condition gives a negative electron temperature. Pressure balance would be achieved if the electron temperature were 50% higher on side 2 than on side 1, but this is unlikely.

We conclude that the discontinuity which passed Pioneer 6 at 0109 UT on January 19 1966, was a reverse slow shock.

A Forward Slow Shock. Figure 3 and 4 shows a discontinuity which has the signature of a forward slow shock, namely, an increase in n, T and V and a decrease in B. It was seen at Pioneer 6 at 1423 U.T. on January 20, 1966. The observed parameters and changes are consistent with the Rankine-Hugoniot equations, as indicated by the close agreement between the observed values and a solution to the R-H equations found by Chao's procedure. The "predicted" values of $\underset{\sim}{V}_2$ are in good agreement with the observed values (Table 2).

The shock normals and speeds are given in Table 3, which also shows $V^*_{n_1}$ and $V^*_{n_2}$, the normal flow speeds relative to the shock. Note that $V^*_{n_2} < V^*_{n_1}$ case, indicating that the fluid was decelerated in the shock front. The Mach numbers, M_A and M_{slow}, computed from the numbers in Table 1, are shown in Table 4. They show the characteristics required for a slow shock. Computed estimates of the electron temperatures are also given in Table 4; it can only be said that they have the correct order of magnitude.

All the available evidence suggests that the discontinuity in Figures 3 is a forward slow shock

V. Electron Temperature

Many of the discontinuities which we found in our search for shocks did not satisfy some of the necessary conditions for shocks, and are thus probably tangential discontinuities or rotational discontinuities. The pressure is constant across both tangential and rotational discontinuities. This condition can be used to solve for the electron temperature.

Measurements of the electron temperature near 1 AU, by Montgomery et al. (1968), showed that T_e remains in the range of 10^5 to 1.5×10^{5}°K even though the proton temperature varies from 3×10^{4}°K to 10^{5}°K. These "direct" measurments are based on a fit to a segment of the Maxwellian distribution. At low energies the spectrum is contaminated by photoelectrons from the spacecraft and there is a non-Maxwellian tail at high energies, so there is the possibility of some uncertainty in the direct measurements.

An indirect method of measuring electron temperature, based on the pressure balance at tangential discontinuities, was introduced by Burlaga (1968), who found $T_e \approx 10^{5}$°K. Although this is consistent with the direct measurements it was based on preliminary proton temperatures which were near the threshhold of the detector. Ogilvie and Ness (1969) introduced another indirect method, which gives T_e/T_{ion}; however, they did not give an electron temperature.

Since it is desirable to confirm the direct measurements by a method which is not affected by the photo sheath or non-Maxwellian tail, we have extended the method of Burlaga (1968), using the discontinuities that we have found in the search for shocks.

PRECEDING PAGE BLANK NOT FILMED

Pressure balance gives the following condition

$$\left(\Sigma \; n_i k T_{i\perp} + \frac{B^2}{8\pi}\right)\Bigg|_1^2 = 0 \qquad (1)$$

We do not have measurements of alpha particles, but for an estimate of the average electron temperature it is sufficient to use the average values, $n_\alpha/n_p = .045$ and $T_\alpha/T_p = 3.5$ (Hundhausen, 1968), since the contribution of the alphas to the pressure is relatively small. The measured proton temperature is that along the earth-sun line, T_r, while the appropriate temperature in (1), $T_\perp$, generally differs from this value because of the proton anisotropy, $T_\parallel/T_\perp \approx 1.9$ (Hundhausen, 1968). Since the discontinuity surfaces are usually along the spiral direction (Burlaga, 1968), we may set $T_r \approx 1.5 T_\perp$. This leaves 2 unknowns, T_{e1} and T_{e2}. As a zeroth approximation we assume that $T_{e1} \approx T_{e2}$. This is consistent with the observations of Montgomery et al. (1968) which show that the shape of the Maxwellian part of the spectrum does not change appreciably with time. With $T_{e1} = T_{e2} \equiv T_e$, (1) then gives

$$T_e \, {}^{\circ}K \times 10^{-3} = .044 \, \frac{(n_2 w_2^2 - n_1 w_1^2)}{n_1 - n_2} + \frac{B_2^2 - B_1^2}{.0378(n_1 - n_2)} \qquad (2)$$

where w is the most probable thermal speed $w = \sqrt{2kT/m}$ in km/sec, n is in cm , and B is in units of 10 gauss. Clearly, (2) is applicable only when $n_1 \neq n_2$, and the result is meaningful only if the uncertainty in T_e is relatively small. T_e is relatively small.

The discontinuities for the calculation of T_e were selected from the total set described in Section II by eliminating those which were identified as shocks and those for which the uncertainty in T_e was large as a result of the accumulation of errors in (2). Our crit ion

for a large uncertainty is that T_e determined from (2) with $|\Delta B|/B=.1$, $|\Delta n|/n=.2$, and $|\Delta T|/T=.3$, is greater than $.5 \times 10^{5}$°K. This left 31 discontinuities from which we obtained the distribution of electron temperatures shown in Figure 4a. The most probable value and the average value are both 1.8×10^{5}°K. The width of the distribution is probably statistical rather than real and due to the propagation of errors in the many algebraic operations in (2). The half width at half maximum 10^{5}°K gives a measure of the spread in T_e. Since there are 31 measurements of T_e, the uncertainty of the average is $\pm 2 \times 10^{4}$°K. Thus using the formal criterion $|\Delta T| \leq 5 \times 10^{4}$°K we obtain $T_e = (1.8 \pm .2) \times 10^{5}$°K. A more restrictive criterion for ΔT gives a somewhat smaller value of T_e.

The above method for estimating T_e has 2 difficulties: 1) it assumes that $T_{e1} = T_{e2}$, and 2) it is very sensitive to errors in n, w, and B so that only a fraction of the discontinuities can be used to calculate T_e. As an alternative method, we assumed that $T_{e1} = 10^{5}$°K or 2×10^{5}°K and solved (1) for T_{e2} in each case. The resulting distributions of T_{e2} are shown in Figure 4b and 4c. In both cases, the median value of T_{e2} (calculated) $\approx T_{e1}$ (assumed), consistent with our earlier assumption that the electron temperature usually does not change across a discontinuity. As in Figure 4a, the spread in the distributions is probably due to the propagation of errors. In any case, the symmetry of the distributions in Figure 4b and 4c implies that T_e does not preferentially increase or decrease across the

discontinuities and the width of the distributions gives an upper limit, $|\Delta T_e| < 10^5$ °K, for the change in the temperature across a discontinuity.

V . Summary

We have searched through Pioneer 6 data for 3 data for reverse fast shocks, and forward and reverse slow shocks. No reverse fast shocks were found. A reverse slow shock was identified; such a shock has not been reported heretofore. A forward slow shock was also identified and was found to be similar to the two found early by Chao and Olbert (1970).

Numerous (50) other discontinuities were found, most of which are probably tangential since all of the plasma parameters (n, V, T) changed across most of them. In particular, changes in B were essentially always accompanied by changes in n, which indicates that discontinuities of the type suggested by Ivanov (with $B_2/B_1 \neq$, $n_2/n_1 = 1$) seldom if ever occur in the solar wind. More precisely, in a sample of discontinuities in B from $\approx$ 4 months of data from Pioneer 6, <5% were associated with no density change, i.e., <5% were the type of discontinuities predicted by Ivanov.

Assuming that the non-shock discontinuities were either tangential or rotational and assuming no change in the electron temperature T_e across the discontinuities, one can use the pressure balance condition to calculate T_e. Using those discontinuities for which we could compute reasonably accurate ($\pm$50%) values of T_e we obtained an average $T_e = (1.8 \pm .2) \times 10^5 {}^oK$ from 31 of the discontinuities. This is in good agreement with the directly measurements values.

ACKNOWLEDGEMENTS

The magnetic field data for this study are from the experiment: of Dr. N. F. Ness. The plasma data are from the M.I.T. experiment . special thanks are due to A. Lazarus, J. Binsak, and H. Howe.

One of us, J. Chao thanks Dr. Franco Mariani for his hospitality at the Laboratorio Plasmanello Spazio, (NR, Universita di Roma, Rome, Italy, where J. Chao completed this work. His work was supported on part by NASA Grant Number NGL 22-009-015 and in part by U. S. Air Force contract F 19628-69-C-002.

Helpful discussions with Drs. Ness and Ogilvie are also appreciated.

REFERENCES

Behannon, K. W., K. H. Schatten, D. H. Fairfield, and N. F. Ness, Trajectories of Explorers 33, 34, and 35, July 1966 - April 1969, NASA-GSFC X-692-70-64 1970.

Burlaga, L. F., Microscale structures in the interplanetary medium, Solar Physics, 4, 67, 1968.

Burlaga, L. F., A reverse hydromagnetic shock in the solar wind, Cosmic Electrodynamics, 1, 233, 1970.

Burlaga, L. F., Discussion of a paper by K. G. Ivanov, "Rotational discontinuities in the solar wind", NASA-GSFC X-692-71-74

Chao, J. K., Interplanetary collisionless shock waves, MIT Technical Note CSR TR-70-3, 1970.

Chao, J. K. and J. Binsack, to be published, 1971.

Chao, J. K., and S. Olbert, Observation of slow shocks in interplanetary space, J. Geophys. Res., 75, 6394, 1970.

Colburn, D. S. and C. P. Sonett, Discontinuities in the solar wind, Space Sci. Rev., 5, 439-506, 1966.

Hundhausen, A. J., Direct observations of solar wind particles, Space Sci. Rev., 8, 690, 1968.

Hundhausen, A. J., and M. D. Montgomery, Heat conduction and nonsteady phenomena in the solar wind, J. Geophys. Res., in press, 1971.

Ivanov, K. G., Rotational discontinuities in the solar wind, Akademiya nauk SSSR, in press, 1970.

Lazarus, A. J., H. S. Bridge, and J. Davis, Preliminary results from the Pioneer 6 M.I.T. plasma experiment, J. Geophys. Res., 71, 3787, 1966.

Lyon, E. F., H. S. Bridge, and J. H. Binsack, Explorer 35 plasma measurements in the vicinity of the moon, J. Geophys. Res., 72, 6113, 1967.

Ness, N. F., Simultaneous measurements of the interplanetary magnetic field, J. Geophys. Res., 71, 3319, 1966.

Ness, N. F., C. S. Scearce, and S. Cantarano, Preliminary results from the Pioneer 6 magnetic field experiment, J. Geophys. Res., 71, 3305, 1966.

Ness, N. F., K. W. Behannon, C. S. Scearce, and S. C. Cantarano, Early results from the magnetic field experiment on lunar Explorer 35, J. Geophys. Res., 72, 5769, 1967.

Montgomery, M. D., S. J. Bame, and A. J. Hundhausen, Solar wind electrons: Vela 4 measurements, J. Geophys. Res., 73, 4999, 1968.

Montgomery, M. D., J. R. Asbridge, and S. J. Bame, Vela 4 plasma observations near the earth's bow shock, J. Geophys. Res., 75, 1217, 1970.

Ogilvie, K. W. and N. F. Ness, Dependence of the lunar wake on solar wind plasma characteristics, J. Geophys. Res., 74, 4123, 1969.

FIGURE CAPTIONS

Figure 1 Distribution of B_1/B_2, n_1/n_2 and w_1/w_2 for discontinuities selected from Pioneer 6. The dip in the distribution of B_1/B_2 is due to the selection procedure which eliminates discontinuities with small changes in B. The n_1/n_2 distribution indicates that discontinuous changes in B are essentially always accompanied by changes in n. The lowest histogram shows that the temperature (thermal speed, w) tends to change also; it is not known to what extent the width of this distribution is determined by measurement uncertainties.

Figure 2 Reverse slow shock of 19 January, 1966. Plasma and magnetic field measurements are shown together with best fits (solid lines) to the Rankine-Hugoniot equations, determined by Chao's procedure.

Figure 3 Forward slow shock (See Figure 2).

Figure 4 Computed electron temperatures. a) Distribution of temperatures computed from the pressure balance condition on the assumption that $T_{e1} = T_{e2} = T_e$ and the requirement that $\Delta T_e \lesssim 5\times10^4\,^oK$. b) Distribution of temperatures T_{e2} computed assuming that $T_{e1} = 10^5\,^oK$. c) Distribution of temperatures T_{e2} computed assuming that $T_{e1} = 2\times10^5\,^oK$.

TABLE 1

BEST-FIT VALUES*

Time		B_{1R}	B_{1T}	B_{1N}	B_{2R}	B_{2T}	B_{2N}	B_1	B_2	V_{1R}	V_{1T}	V_{1N}	V_{2R}	V_{2T}	V_{2N}	V_1	V_2	n_1	n_2
19 Jan.	0109	4.4	-2.0	-0.2	4.0	-1.0	1.0	5.2	4.2	321	15	15	310	25	22	323	311	7.0	9.0
20 Jan.	1423	-5.0	6.0	-4.0	-4.5	1.8	-3.6	10.0	6.0	388	13	-10	405	-30	4	388	406	7.5	10.0
Oct.	0819	3.2	-9.7	-5.9	4.8	-2.3	-0.8	11.8	5.5	3[illegible]	[illegible]	3[illegible]	3[illegible].8	56	87	348	363	4.8	[illegible]

*Here B is in $\gamma=10^{-5}$ gauss, V is in km/sec, and n is in cm^{-3}.

TABLE 2

$\underset{\sim}{V}_2$, Predicted and Observed

Date	V_2	V_{2R}	V_{2T}	V_{2N}	km/sec
January 19	312	311	25	23	Theory
0109 UT	314 ± 5	310 ± 5	18 ± 10	5 ± 20	Observed
January 20	406	405	-28	4	Theory
1423 UT	415 ± 10	414 ±10	-10 ± 15	0 ± 20	Observed
October 27	363	348	56	87	Theory
0819	359 ± 10	348 ± 10	55 ± 10	69 ± 20	Observed

TABLE 3

BASIC SHOCK PARAMETERS

	January 19, 1966	January 20, 1966
$\underset{\sim}{V}_s$ (km/sec)	(212,1,135)	(241,95,193)
V_s (km/sec)	251	323
$\hat{n}$ (RTN)	(.85, .01, .54)	(.75, .30, .60)
$\hat{n}$ (θ_s, ϕ_s)	$\theta_s = 33^\circ$, $\phi_s = 0^\circ$	$\theta_s = 37^\circ$, $\phi_s = 22^\circ$
V_{n1}*(km/sec)	-29	37
V_{n2}*(km/sec)	-23	27
$\theta_{B,n}$	42°	60°

TABLE 4

ADDITIONAL SHOCK PARAMETERS

	January 19, 1966	January 20, 1966
$M_{A,1}$	.9	.9
$M_{A,2}$	.8	.8
$M_{slow,1}$	1.2	1.3
$M_{slow,2}$	0.8	0.8
$T_{e1}(10^5 {}^oK)$	≈ 4	≈ 4
$T_{e2}(10^5 {}^oK)$	≈ 6	≈ 11

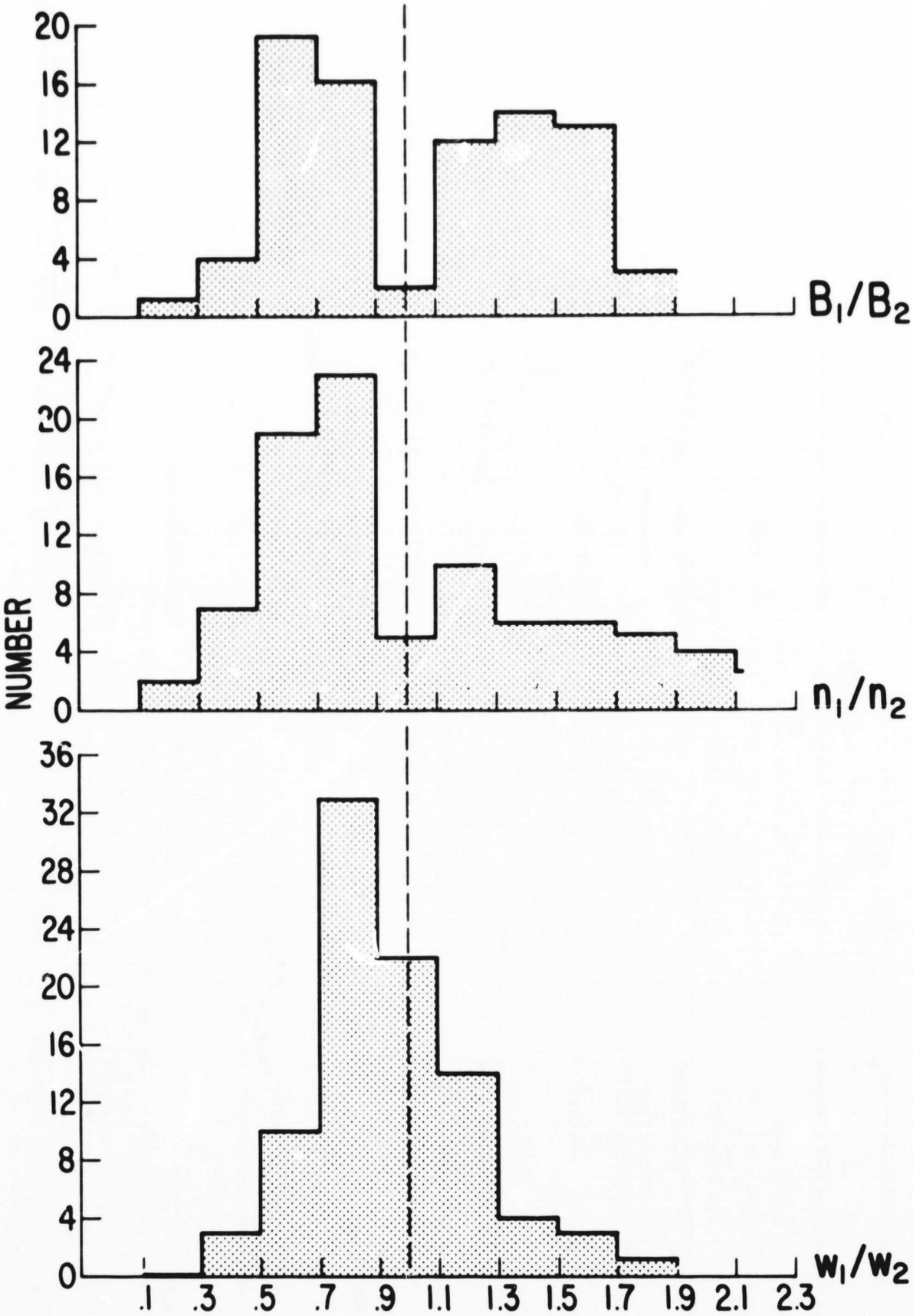
NUMBER
B_1/B_2
n_1/n_2
w_1/w_2
0
4
8
12
16
20
24
28
32
36
.1
.3
.5
.7
.9
1.1
1.3
1.5
1.7
1.9
2.1
2.3

Figure 1

REVERSE SLOW SHOCK
JANUARY 19, 1966
PIONEER 6

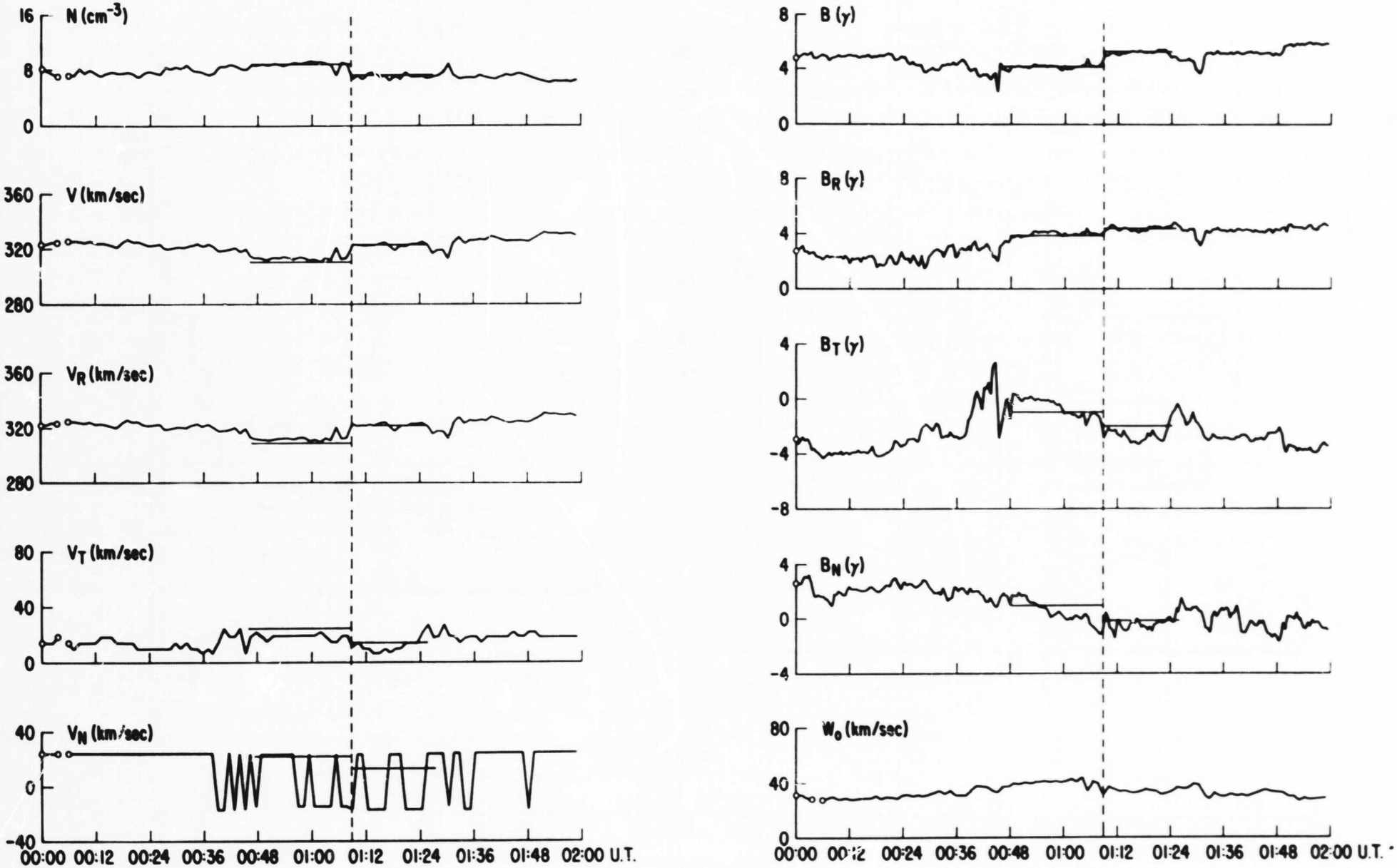

Figure 2

FORWARD SLOW SHOCK
JANUARY 20, 1966
PIONEER 6

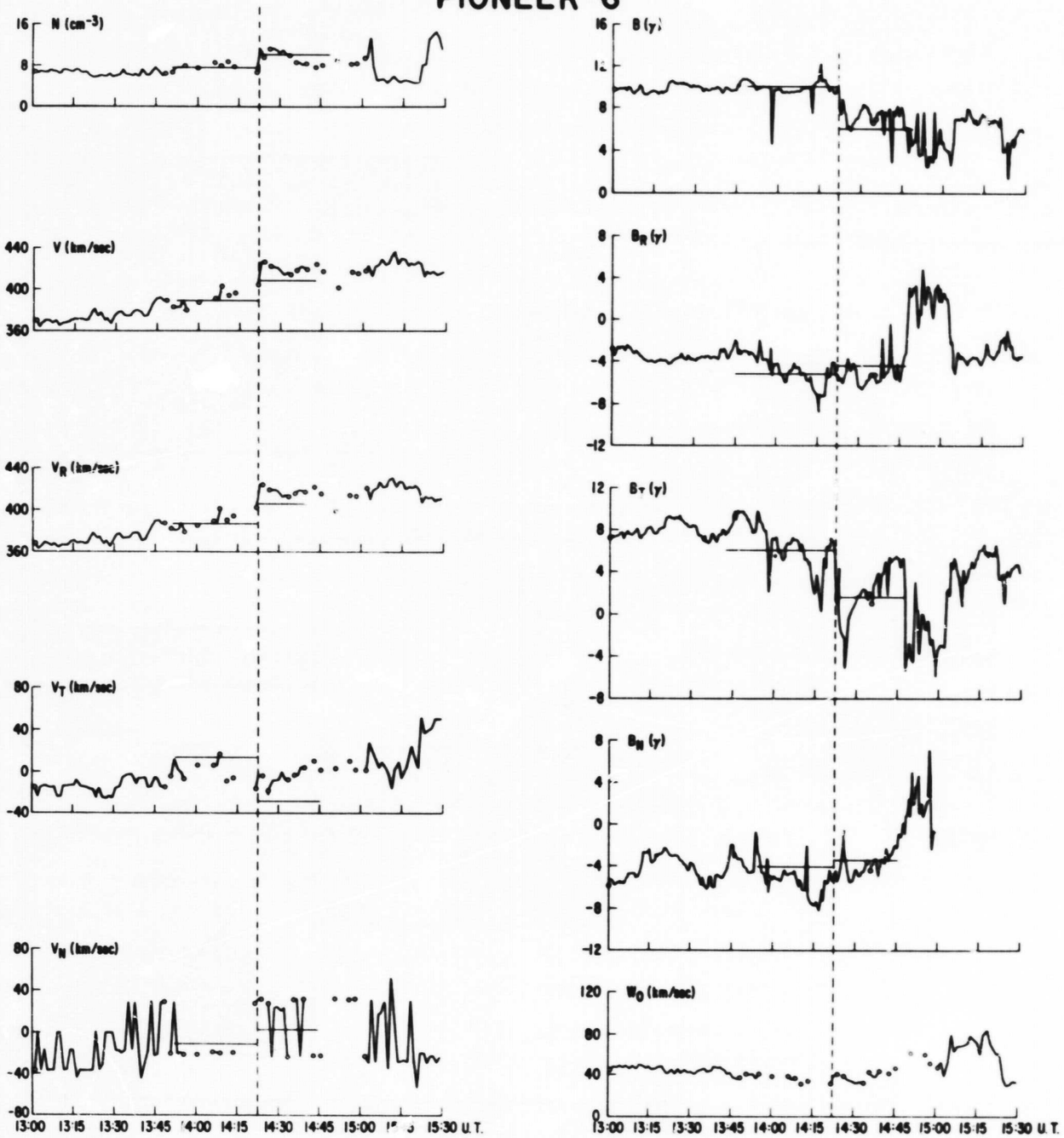

Figure 3

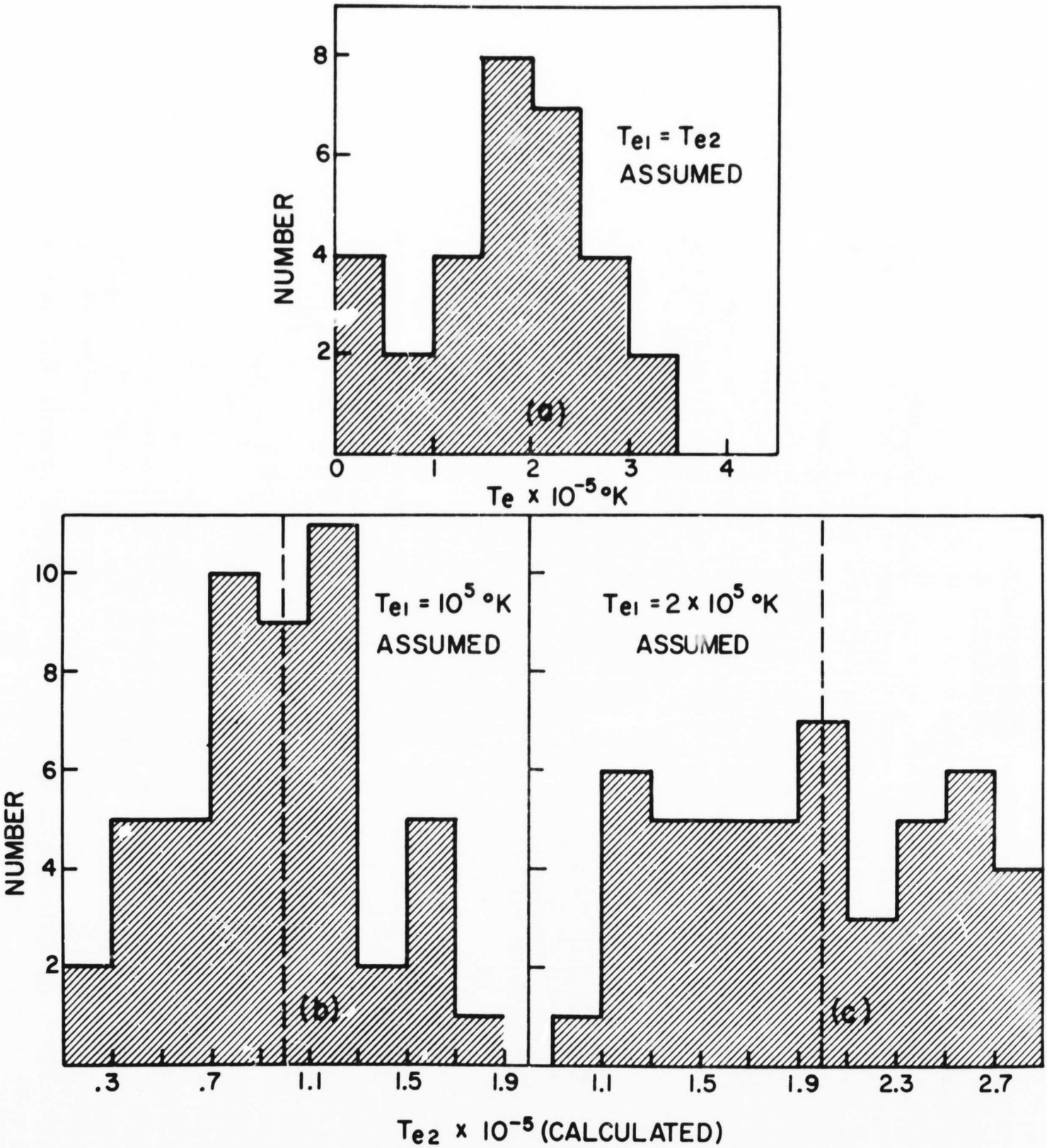
NUMBER
8
6
4
2
Te1 = Te2
ASSUMED
(a)
0
1
2
3
4
Te x 10^-5 °K
NUMBER
10
8
6
4
2
Te1 = 10^5 °K
ASSUMED
(b)
.3
.7
1.1
1.5
1.9
Te1 = 2 x 10^5 °K
ASSUMED
(c)
1.1
1.5
1.9
2.3
2.7
Te2 x 10^-5 (CALCULATED)

Figure 4